Plant Soil
https://doi.org/10.1007/s11104-025-08085-z

RESEARCH ARTICLE

Redistribution of major mineral-forming elements (Fe, Al, Si, Mn) and nutrient-associated trace elements (Cu, Zn, P) following rice-to-pomegranate land-use conversion in Southern Italy

Veronika Cyprichová · Antonio Gelsomino · Marcel B. Miglierini · Marek Bujdoš · Beatrix Petrovičová · Martin Urík

Received: 4 August 2025 / Accepted: 3 November 2025
© The Author(s) 2025

Abstract

Aims This study explores the geochemical consequences of converting long-term flooded rice fields to non-flooded pomegranate orchards in calcareous, organic-rich soils of Southern Italy.

Methods By analyzing topsoil (0–20 cm) and subsoil (50 cm) samples, we investigated how land-use change influences the distribution, speciation, and mobility of iron, copper, zinc, manganese, aluminum, phosphorus, and silicon. Sequential extraction, Mössbauer spectroscopy, and elemental analyses were employed to assess shifts in redox-sensitive mineral phases and nutrient pools.

Results The transition to aerobic conditions induced substantial alterations in iron fractionation, including the loss of amorphous and acid-soluble phases and increased crystallization into more stable reducible forms. Despite these structural changes, Mössbauer spectroscopy revealed that iron redox states remained largely unaffected, indicating strong valence-state resilience. Copper became more strongly associated with manganese and (amorphous) iron oxides, while its acid-soluble fraction declined significantly, particularly in the subsoil. In contrast, zinc remained largely immobilized within the residual fraction, demonstrating greater geochemical stability.

Conclusions Our findings underscore the complex interaction between redox conditions, mineral transformations, and nutrient dynamics during land-use transitions. Understanding these processes is critical for managing soil fertility and minimizing environmental risks in Mediterranean agroecosystems.

Keywords Agricultural soil management · Iron fractionation · Paddy soils transformation · Trace elements mobility

Responsible Editor: Juan Barcelo.

V. Cyprichová · M. Bujdoš · M. Urík (✉)
Institute of Laboratory Research On Geomaterials, Faculty of Natural Sciences, Comenius University, Mlynská Dolina, 84215 Bratislava, Slovakia
e-mail: martin.urik@uniba.sk

A. Gelsomino · B. Petrovičová
Department of Agricultural Sciences, Mediterranean University of Reggio Calabria, Feo di Vito, 89124 Reggio Calabria, Italy

M. B. Miglierini
Institute of Nuclear and Physical Engineering, Slovak University of Technology, Ilkovičova 3, 841 04 Bratislava, Slovakia

M. B. Miglierini
Department of Nuclear Reactors, Faculty of Nuclear Sciences and Physical Engineering, Czech Technical University, V Holešovičkách 2, 18000 Prague, Czech Republic

Introduction

Soil redox dynamics play a pivotal role in the speciation, mobility, and transformation of both essential

Published online: 19 November 2025

and potentially toxic elements in agricultural soils. Rice paddy soils, in particular, represent unique biogeochemical environments where prolonged water saturation and reducing conditions strongly influence redox-driven transformations of iron (Kögel-Knabner et al. 2010) and associated trace metals such as copper and zinc (Hu et al. 2006). However, the transition from conventional to alternative cropping systems, driven by a growing economic interest in tree crops like pomegranate (*Punica granatum* L.) (Raimondo et al. 2025), introduces substantial changes in soil aeration, redox potential, and microbial activity. These shifts are expected to alter soil chemical properties connected to nutrient availability and metal speciation. Despite this, current research has primarily focused on changes in microbial diversity (Yang and Zhang 2014), soil organic carbon and nitrogen dynamics, and in fertility variables (Nishimura et al. 2008), whereas the effects on iron and trace metal dynamics remain largely underexplored. Iron, in particular, exhibits geochemical behavior that is highly sensitive to environmental conditions such as pH and redox potential (Notini et al. 2023), both of which can fluctuate considerably following changes in soil management. These fluctuations influence not only the speciation and mobility of iron itself but also affect the fate of other micronutrients. Iron oxides and hydroxides serve as key sorbents in soils, sequestering trace elements such as zinc and copper (Liu et al. 2014), thereby significantly impacting their bioavailability.

This study aims to fill this knowledge gap by evaluating the impact of land management change (from flooded rice to non-flooded pomegranate cultivation) on the distribution and speciation of iron, copper and zinc in calcareous paddy soils, located in the coastal plain of Sibari, Calabria, Italy. We investigated both topsoil and subsoil profiles, recognizing that microbial activity, organic carbon turnover, and redox fluctuations vary with soil depth. To achieve this aim, we integrated six- step sequential extraction, Mössbauer spectroscopy, and elemental analyses to determine the partitioning and valence state of iron and trace metals (copper and zinc) distribution and primary soil associations across different fractions. To identify the key pedogeochemical mechanisms underlying metal redistribution, the changes in dissolved organic carbon, calcium carbonate content, and the partitioning of phosphorus, manganese, aluminum and silicon were also monitored to assess their role in driving or moderating iron and trace element mobility. We expect that these findings contribute to a better understanding of soil geochemistry in Mediterranean agroecosystems undergoing land-use change, with implications for nutrient management and environmental sustainability.

Materials and methods

Soils sampling and characterization

The paddy soil samples were collected from adjacent fields within the farm Società Agricola Terzeria s.r.l. Soc. Benefit (39°46′39′′N, 16°27′00′′E) during the 2022/2023 growing season. The farm is located in the costal lowland of Crati river in Southern Italy (Sibari Plain, Cosenza, Calabrian Region) (Fig. 1). These fields had been continuously cultivated with rice (*Oryza sativa* L. cv *Karnak*) for past 25 years, remaining flooded for most of the year. However, cultivation practices and type of planted crops have since diverged across different parts of the rice fields. The first experimental section remained unchanged, continuing under predominantly reductive conditions (**RiceF**). The second experimental section underwent cultivation with pomegranate trees for five years (**PomF**).

As depicted in Fig. 1, five topsoil samples were collected from the A horizon at a depth of 20 cm in each field, along with one subsoil sample from a depth of 50 cm. All moist soil samples were air-dried in the laboratory and sieved through a 2 mm mesh. A portion of the sieved soil was further finely ground and passed through a 0.16 mm pore size mesh. These soil fractions were subsequently used for the analysis of chemical and textural properties and for the sequential extraction procedure.

Soil physical and chemical properties (texture, pH, EC, total and active $CaCO_3$, organic carbon (total and dissolved), total nitrogen, C/N, CEC) was determined according to the standard methods recommended by the Soil Science Society of America (Klute 1986; Sparks et al. 2001). Readily available silica was measured in the extract using 0.01 M solution of $CaCl_2$ according to method Haysom and Chapman (1975). Exchangeable silica released by dissolving amorphous iron or manganese soil phases, was extracted

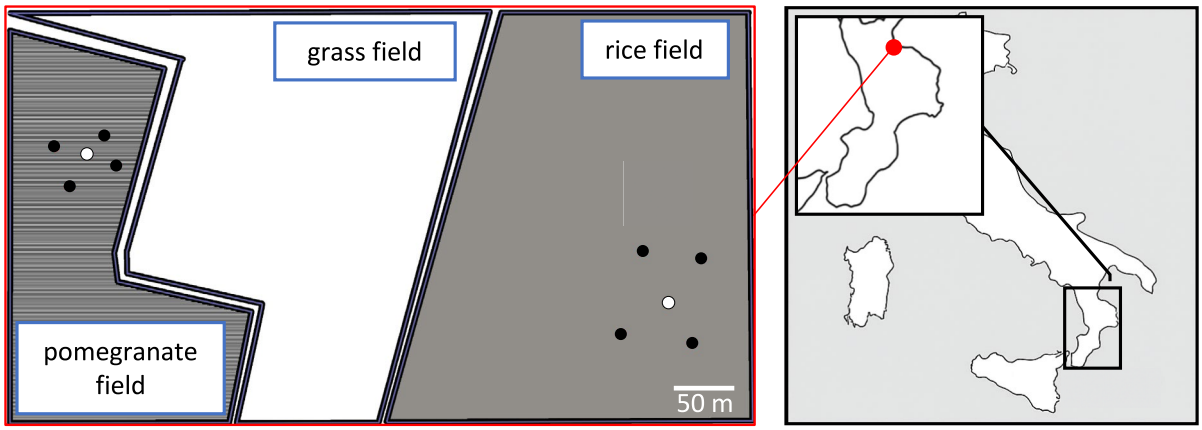

Fig. 1 Map illustrating the locations of sampling sites. Black dots denote samples collected at a depth of 20 cm, while white dots mark sites where samples were collected from both 20 cm and 50 cm depths

into a solution of ammonium oxalate monohydrate and oxalic acid, as described in the Tamm (1922). DeMaster (1981) methodology was used to measure the content of biogenic and mineral forms of silica.

Sequential extraction procedure

There are several modifications of one-step and sequential extraction procedures used to determine the reactive and bioavailable fractions of elements in soils and sediments, as well as their primary associations (Hagarová 2015; Nemček and Hagarová 2021). In this study, a six-step sequential extraction procedure, as described by Alan and Kara (2019), was performed in triplicate for each soil sample. This approach aimed to investigate the distribution of iron, manganese, aluminum, silicon, copper, zinc, and phosphorus across the following soil fractions:

(1) water soluble and exchangeable fraction: a 0.5 g soil sample (< 0.16 mm particle size) was combined with 20 mL of 20 mmol·L^{-1} $CaCl_2$ (pH 6.5) in a 50 mL centrifuge tube. The mixture was then shaken for 16 h at room temperature (25 °C) on an overhead rotary shaker at 40 rpm. The extracts were separated from the solid phase by centrifugation at 6000 rpm for 30 min. The supernatants were collected and stored in centrifuge tubes at 4 °C prior to analysis. After decanting the extract, the remaining residue was washed with double-distilled water, centrifuged again at 6000 rpm for 30 min, and the supernatant was discarded. The residue was then used for the next step.
(2) acid-soluble, carbonate associated fraction: the residue from step (1) was mixed with 20 mL of 0.1 mol·L^{-1} HCl (pH 1.5). The mixture was shaken for 16 h at room temperature (25 °C) on an overhead rotary shaker at 40 rpm. The extracts were separated by centrifugation at 6000 rpm for 30 min, and the supernatants were collected and stored as described in step (1). The solid residues were washed as in step (1) before proceeding to step (3).
(3) reducible fraction, bound to manganese oxides: the residue from step (2) was mixed with 20 mL of 0.1 mol·L^{-1} $NH_2OH.HCl$ (pH 2). The mixture was shaken for 16 h at room temperature (25 °C) on an overhead rotary shaker at 40 rpm. The extracts were separated by centrifugation at 6000 rpm for 30 min, and the supernatants were collected and stored as described in step (1). The solid residues were washed as in step (1) before proceeding to step (4).
(4) acidic oxalate soluble fraction, bound to amorphous iron bearing minerals: the residue from step (3) was mixed with 20 mL of a mixture of 0.2 mol·L^{-1} $(NH_4)_2C_2O_4$ and 0.2 mol·L^{-1} $H_2C_2O_4$ (pH 3). The mixture was shaken for 16 h at room temperature (25 °C) on an overhead rotary shaker at 40 rpm. The extracts were separated by centrifugation at 6000 rpm for 30 min, and the supernatants were collected and stored

as described in step (1). The solid residues were washed as in step (1) before proceeding to step (5).

(5) acidic citrate-soluble fraction bound to crystalline iron bearing minerals: the residue from step (4) was mixed with 20 mL of 0.2 mol·L^{-1} Na-citrate, 0.05 mol·L^{-1} citric acid and 0.1 mol·L^{-1} $Na_2S_2O_3$. The mixture was shaken for 16 h at room temperature (25 °C) on an overhead rotary shaker at 40 rpm. The extracts were separated by centrifugation at 6000 rpm for 30 min, and the supernatants were collected and stored as described in step (1). The solid residues were washed as in step (1) before proceeding to step (6).

(6) oxidizable fraction, bound to organic matter and sulfides: the residue from step 5 was mixed with 8.8 mol·L^{-1} hydrogen peroxide (pH 2–3) and after the reaction and evaporation of peroxide the extraction was continued with 25 mL of 3.2 mol·L^{-1} ammonium acetate prepared in 25% HNO_3. The mixture was shaken for 16 h at room temperature (25 °C) on an overhead rotary shaker at 40 rpm. The extracts were separated by centrifugation at 6000 rpm for 30 min, and the supernatants were collected and stored as described in step (1). The solid residues were washed as in step (1) before proceeding to step (7).

(7) residual fraction: the non-dissolved residue from step (6) was digested in PTFE pressure vessels in microwave digestion system Anton Paar Multiwave 3000 using concentrated HNO_3 and H_2O_2 (4 + 2 mL) at pressure of 60 bar. After digestion 5 mL of HCl and 1 mL of HF were added and solutions were made up to 50 mL.

Water-extractable inorganic nutrients

Readily available nutrients (lithium, sodium, ammonium, potassium, magnesium, calcium, fluoride, nitrate, nitrite, chloride, sulfate) were water-extracted (substrate/water, 1/10, w/v) under horizontal shaking at room temperature for 2 h, centrifuged at 5,000 g for 5 min and then filtered through Whatman™ n. 42 filter paper. Filtrates were passed through a 0.22 μm Millipore™ filter and stored at −20 °C before ion chromatographic analysis.

Analytical procedures

To determine the concentration of iron, aluminum, silicon, copper, zinc and manganese in collected RiceF and PomF soil samples and their extracts, a flame atomic absorption spectrometer (PerkinElmer 1100, USA) with an air-acetylene flame (air flow rate 8.0 L·min^{-1}, acetylene flow rate 2.5 L·min^{-1}) was used. The phosphorus content was analyzed using inductively coupled plasma optical emission spectroscopy (ICP-OES), with an ICP spectrometer (Jobin Yvon 70 Plus, France) equipped with a concentric nebulizer (Meinhard, USA) and a cyclonic spray chamber. The plasma power was set to 1000 W. The limit of quantification for the iron, aluminum, silicon, copper, zinc, manganese and phosphorus for the selected methods were 0.01 mg·L^{-1}, 0.1 mg·L^{-1}, 0.1 mg·L^{-1}, 0.005 mg·L^{-1},0.005 mg·L^{-1}, 0.01 mg·L^{-1}, and 0.5 mg·L^{-1}, respectively. Calibration solutions were prepared from CertiPUR ICP 1000 mg·L^{-1} single-element standard solutions (Merck, Germany). Analytical procedure accuracy was tested by analyses of certified reference materials (CRM) Astasol AN9098MN (Analytika, Czech Republic).

Inorganic cations and anions were determined by ion chromatography using a Dionex™ ICS 1100 (Dionex Corp., USA) equipped with an isocratic pump, a conductivity detector, and an auto-sampler (Dionex™ AS-DV, ThermoFisher Scientific, USA). Cations were determined using a self-generating CDRS-600 suppressor (4 mm) (ThermoFisher Scientific), an analytical column (4 mm ID × 250 mm) Dionex™ IonPack™ CS12A RFIC™ (Dionex Corp.), and an eluent solution (20 mM methane sulfonic acid) at a flow rate of 1.2 mL·min^{-1}. Anions were determined using a self-generating AERS-500 suppressor (4 mm) (ThermoFisher Scientific), an analytical column (4 mm ID × 250 mm) Dionex™ Ion-Pac™ AS22 RFIC™ (Dionex Corp.), and an eluent solution (3.5 mM sodium-carbonate/1.0 mM sodium-bicarbonate) at a flow rate of 1.2 mL·min^{-1}. Instrumental control and chromatographic data processing was done by the Thermo Scientific Dionex Chromeleon Chromatography Data System 7.2 (ThermoFisher Scientific).

The ^{57}Fe Mössbauer spectroscopy was used to identify any structural changes of iron in the soil samples collected from rice and pomegranate fields. ^{57}Fe

Mössbauer spectroscopy was applied in the transmission geometry. The ^{57}Co(Rh) source of γ radiation was kept at room temperature; and conventional spectrometer (WissEl, GmbH, Germany) working in constant acceleration mode was used. Calibration of the velocity scale was performed by an α-Fe foil at room temperature. The spectra were analyzed using Confit program.

All statistical and data analysis regarding the extraction experiments were conducted using the Analysis ToolPak add-in program in MS Office Excel (Microsoft, USA).

Results

Soil characteristics

The studied agricultural soil belongs to the textural class of silty clay loam and contains 17.6% sand, 52.4% silt, and 30.0% clay. According to the WRB the soil was classified as Calcari-Gleyic Fluvisol. Soil samples from adjacent fields of two different agricultural systems: a rice field (RiceF) and a pomegranate field (PomF) were collected at depth of 0–20 cm and 50 cm and their pedochemical characteristics were compared (Table 1). The pH values indicate slightly alkaline conditions in both fields, with minor variations between depths. The total nitrogen content is higher in the PomF compared to the RiceF, but decreases significantly at depth. The content is higher in the PomF indicating accumulation over time. The total silicon content remained stable across sites, while iron and aluminum were lower in the PomF. Our experimental results indicate significant shifts in both total and dissolved organic carbon, highlighting the changes in the studied paddy soil management affected the organic carbon storage potential of the soil. Interestingly, the transformation in management led to enrichment of topsoil with both organic carbon and total organic carbon, while the subsoil organic carbon has significantly decreased. Total copper and zinc levels in soil declined over time. An increase in total phosphorus is observed in the topsoil of the PomF, while its content decreases in the subsoil following changes in soil management. However, within the soil profile, total phosphorus content decreases with depth for both RiceF and PomF, indicating its limited mobility. The observed variations in the contents of selected elements in the studied soils are listed in Table 1.

Table 1 Pedochemical characteristics of sampling sites, including total content of the studied metals in soil samples. Samples collected from the rice field represent the initial state, while those from the field cultivated with pomegranate represent the five-year aging point

Soil variable	Rice field		Pomegranate field	
	Sampling depth (cm)			
	0–20	50	0–20	50
pH_{H2O}	7.70	7.79	7.59	7.79
pH_{CaCl2}	7.27	7.30	7.00	7.22
EC (μS cm^{-1})	384	314	234	250
$CaCO_3$ (%)	7.7	9.0	14.6	19.9
TOC (%)	1.94	1.63	2.24	1.03
DOC (μg g^{-1})	62.6	81.9	88.5	25.1
CEC (cmol kg^{-1})	19.5	19.5	20.8	14.7
Tot C (mg g^{-1})	19.4	16.3	22.4	10.3
Tot N (mg g^{-1})	1.59	1.20	1.65	0.56
C/N	12.2	13.6	13.6	18.3
Tot Si (%)	25.3	26.1	22.6	21.1
Tot Fe (%)	4.10	4.10	3.68	3.37
Tot Mn (%)	1.29	1.37	1.35	1.36
Tot Cu (μg g^{-1})	50.5	49.5	46.3	38.9
Tot Zn (μg g^{-1})	121	119	114	87
Tot P (μg g^{-1})	711	574	867	370

Analysis of water-soluble cations and anions concentrations revealed differences related to crop cultivation and depth (Table 2). The PomF field consistently exhibited higher concentrations of sodium, potassium, calcium, and chloride water-extractable ions in both topsoil and subsoil samples. These differences suggest that the shift in crop cultivation, along with seawater intrusion onto the soil surface during dry periods, influenced the distribution of these ions. Conversely, the concentrations of sulfides, fluoride, and magnesium water-extractable ions decreased in the PomF field following the change in cultivation, in both surface and subsurface horizons. The concentration of lithium, ammonium and nitrate water-extractable ions remained the same.

Table 2 Effect of crop cultivation and soil depth on the content of extractable ions

	Extractant	RiceF		PomF	
Sampling depth (cm)		0–20	50	0–20	50
Si_{CaCl2} (μg g^{-1})	0.1 M $CaCl_2$	6.0	4.8	10.7	5.8
Si_{oxal} (μg g^{-1})	0.2 M NH_4-oxalate	213	211	198	102
Si_{carb} (mg g^{-1})	0.094 M Na_2CO_3 (85 °C)	43.8	*	33.0	*
Li^+ (μg g^{-1})	water	0.05	0.08	0.07	0.05
Na^+ (μg g^{-1})	water	17.5	50.4	163	177
NH_4^+ (μg g^{-1})	water	22.3	27.7	30.5	31.1
K^+ (μg g^{-1})	water	44.6	56.7	64.6	67.3
Mg^{2+} (μg g^{-1})	water	85.4	141	36.2	35.7
Ca^{2+} (μg g^{-1})	water	204	142	234	238
F^- (μg g^{-1})	water	8.3	6.9	6.0	6.9
Cl^- (μg g^{-1})	water	20.6	20.8	41.7	35.5
NO_2^- (μg g^{-1})	water	4.3	0.3	1.3	0.4
NO_3^- (μg g^{-1})	water	4.1	0.8	27.4	1.9
SO_4^{2-} (μg g^{-1})	water	144	206	29.1	103

* not analyzed

Distribution and speciation of iron

The total iron content in the soils of studied area exhibited significant variation due to changes in soil management (Table 1), with RiceF displaying uniform iron distribution within the soil profile, reaching 4.1% in both topsoil and subsoil soil samples. In contrast, the cultivation of pomegranates led to a progressive decline in total iron content across both soil profiles. The subsoil layer (50 cm depth) proved particularly sensitive to changes in soil management. Notably, five years of pomegranate cultivation resulted in a substantial 18% reduction in total iron content at this depth.

The sequential extraction of iron from the soils revealed that the decline in iron content primarily impacted four soil fractions: the residual (non-soluble silicate) fraction in subsoil, the less crystalline iron (amorphous hydrated oxyhydroxides) fraction, the fraction bound to manganese (hydroxy)oxides (reducible) and the carbonate-associated (acid-soluble) fraction (Fig. 2). While the relative iron content in the subsoil's residual fraction showed a statistically significant increase from 62% in RiceF to 71% in PomF, the acid-soluble and amorphous iron-associated fractions decreased over five years of altered soil management by 97% and 14%, respectively. Similar, though less pronounced, effects were observed in the topsoil samples at a depth of 20 cm, with decreases of 68% in the acid-soluble fraction and 10% in the amorphous iron-associated fraction. Iron content in the reducible fraction increased by 1.3-fold in the topsoil and decreased by 33% in the subsoil following the alteration of soil management practices.

As previously noted, the majority of soil iron was retained in the residual fraction, accounting for 62% to 71% of the total iron content. This was followed by the acidic oxalate-soluble fraction, with a maximum relative content of 14.6%, and the oxidizable fraction (organic matter-associated and sulfide bound iron), with a maximum relative content of 12.4%. The least significant fraction was the water-soluble iron, which accounted for only < 0.05% of the total iron content. This trend has remained consistent, regardless of the sample's position within the soil profile or changes in soil management. Interestingly, most of the extractable iron remained associated with its sulfidic and low-crystalline phases, as well as iron bound to the organic content of the paddy soils, even after five years of altered soil management (Fig. 2). Moreover, no significant changes were observed in the Fe^{2+}/Fe^{3+} distribution within the soil. This was confirmed by Mössbauer analysis of samples from both rice and pomegranate-cultivated soils. The results, illustrated in Fig. 3, reveal the presence of asymmetric overlapping doublets attributed to ferrous and ferric ions occupying octahedral or tetrahedral sites (Table 3).

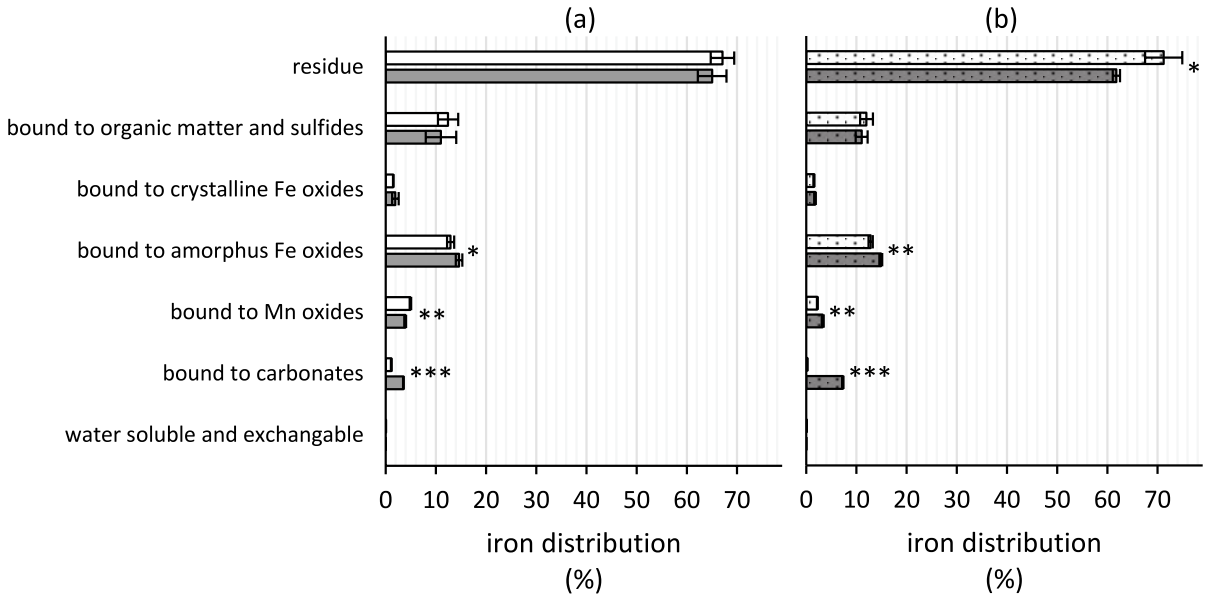

Fig. 2 Distribution of iron in soils collected at (**a**) 20 cm depth (topsoil sample) (**b**) or 50 cm (subsoil sample). The bars of gray and white colors represent samples collected from the rice field, and the field with five-year pomegranate cultivation after discontinued rice cultivation, respectively (bars represent the mean values, and error bars indicate the standard deviation from three independent, parallel runs; where not visible, error bars are present but too small to be distinguished from the mean value; asterisks show statistically significant differences between samples: * $P<0.05$, ** $P<0.01$, and *** $P<0.001$)

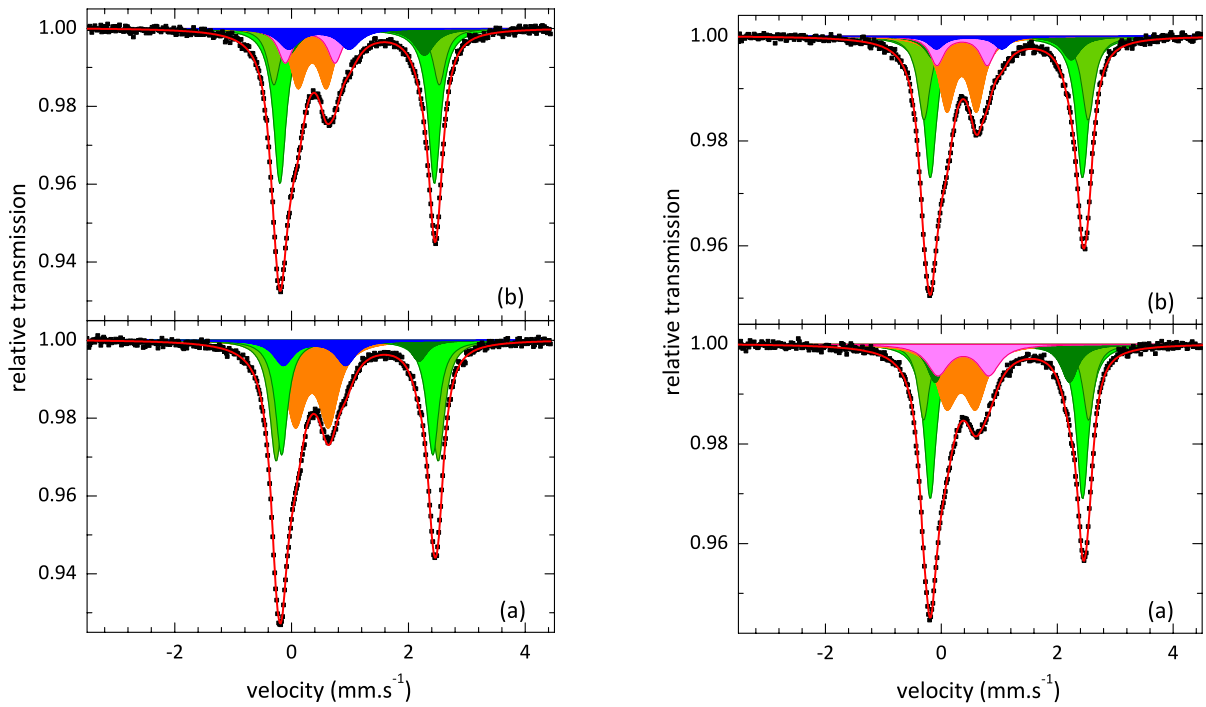

Fig. 3 Mössbauer spectra of (**a**) rice and (**b**) pomegranate fields soil samples collected at (**left**) 20 cm depth (topsoil sample) or (**right**) at 50 cm (subsoil sample)

Table 3 The hyperfine parameters of soil samples collected at rice and pomegranate fields measured at room temperature. The isomer shift is referenced to α-Fe at 295 K. The estimated experimental error margins of relative area *A*, isomer shift *IS*, quadrupole splitting *QS*, and line width Γ are ± 1.5 %, ± 0.02 mm·s^{-1}, ± 0.04 m m·s^{-1}, and ± 0.04 mm·s^{-1}, respectively

sample (depth)	component	*A* (%)	*IS* (mm·s^{-1})	*QS* (mm·s^{-1})	Γ (mm·s^{-1})	site	χ^2
rice field (20 cm)	D1	27	1.124	2.590	0.256	Fe^{2+}, octa	0.91
	D2	29	1.123	2.773	0.268	Fe^{2+}, octa	
	D3	6	1.031	2.303	0.330	Fe^{2+}, octa	
	D4	9	0.393	1.069	0.403	Fe^{3+}, octa	
	D5	0				Fe^{3+}, tetra	
	D6	29	0.349	0.573	0.409	Fe^{3+}, tetra	
pomegranate field (20 cm)	D1	39	1.123	2.646	0.261	Fe^{2+}, octa	0.86
	D2	14	1.114	2.830	0.258	Fe^{2+}, octa	
	D3	11	1.107	2.336	0.416	Fe^{2+}, octa	
	D4	8	0.470	1.036	0.441	Fe^{3+}, octa	
	D5	10	0.320	0.853	0.297	Fe^{3+}, tetra	
	D6	18	0.353	0.487	0.331	Fe^{3+}, tetra	
rice field (50 cm)	D1	36	1.124	2.629	0.253	Fe^{2+}, octa	0.94
	D2	17	1.119	2.844	0.237	Fe^{2+}, octa	
	D3	12	1.054	2.317	0.349	Fe^{2+}, octa	
	D4	0				Fe^{3+}, octa	
	D5	12	0.381	0.882	0.449	Fe^{3+}, tetra	
	D6	23	0.343	0.501	0.434	Fe^{3+}, tetra	
pomegranate field (50 cm)	D1	36	1.123	2.625	0.265	Fe^{2+}, octa	0.86
	D2	21	1.117	2.830	0.260	Fe^{2+}, octa	
	D3	9	1.063	2.358	0.373	Fe^{2+}, octa	
	D4	4	0.481	1.129	0.320	Fe^{3+}, octa	
	D5	8	0.359	0.867	0.295	Fe^{3+}, tetra	
	D6	22	0.351	0.511	0.325	Fe^{3+}, tetra	

The spectra and determined hyperfine parameters suggest that all soil samples contain a similar proportion of Fe^{2+} and Fe^{3+}, as the sum of octahedral Fe^{2+} sites derived from doublets D1-D3 approximates 65% of all iron nuclei, with no statistically significant differences across agricultural management practices or soil profiles due to experimental margin of error. However, changes in cultivation practices resulted in slight rearrangements of Fe^{3+} in octahedral positions, marked by the appearance of component D4 in subsoil soil samples (Table 3). This Fe^{3+} was likely redistributed from tetrahedral positions of less ordered component D5.

At 20 cm soil depth, only a redistribution of Fe^{3+} in tetrahedral positions, represented by components D6 and D5 (Table 3), became evident after five years of altered field management, highlighting the miniscule alterations in arrangement of iron-associated structures and the resilience of both reduced and oxidized iron species in the soil after exposure to altered redox conditions.

Distribution of copper

The total content of copper did not alter significantly within the soil profile in the RiceF, with levels reaching approximately 50 μg·g^{-1} (Table 1). However, the discontinuing flooding and pomegranates cultivation for five years led to changes in copper content at both PomF´s soil depths, with a more pronounced decrease observed at 50 cm depth, where it dropped by 21%, to 38.9 μg·g^{-1} (Table 1).

The alteration in copper content within each soil layer resulted in consistent trends across nearly all soil fractions (Fig. 4), particularly in samples collected at a depth of 50 cm. At this depth, in the PomF sample, changes in soil management led to a significant 75% reduction in relative content of copper

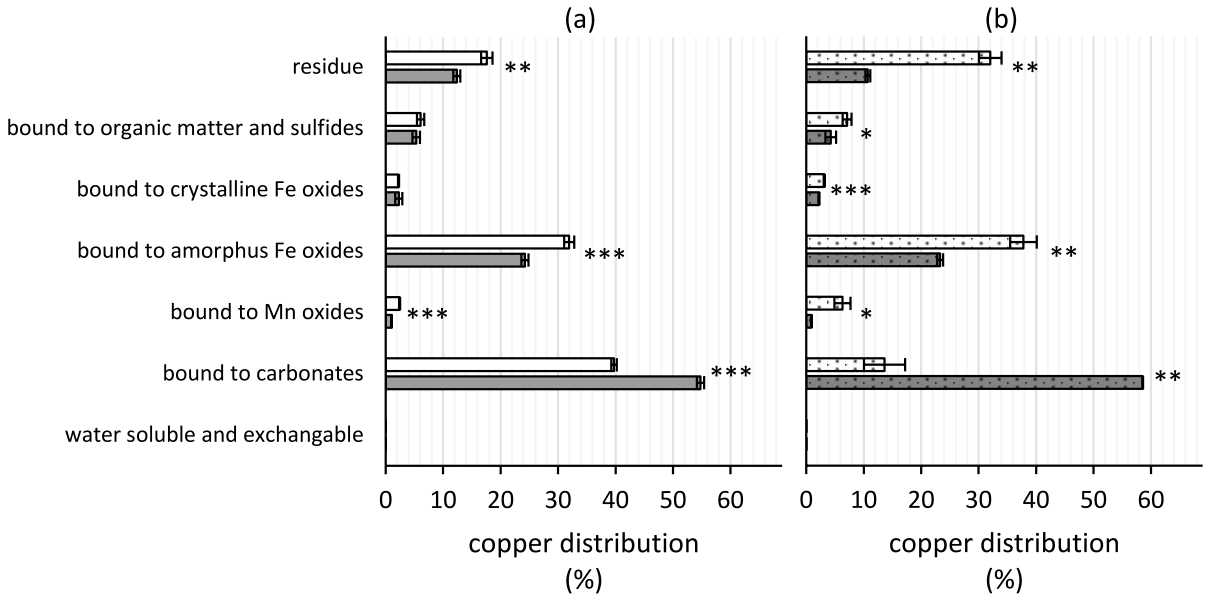

Fig. 4 Distribution of copper in soils collected at (**a**) 20 cm depth (topsoil sample) (**b**) or 50 cm (subsoil sample). The bars of gray and white colors represent samples collected from the rice field, and the field with five-year pomegranate cultivation after discontinued rice cultivation, respectively (bars represent the mean values, and error bars indicate the standard deviation from three independent, parallel runs; where not visible, error bars are present but too small to be distinguished from the mean value; asterisks show statistically significant differences between samples: * $P < 0.05$, ** $P < 0.01$, and *** $P < 0.001$)

associated with the acid-soluble fraction. In contrast, copper bound to amorphous and crystalline hydrous oxides and oxohydroxides of manganese and iron, as well as copper found in the residual fraction, showed statistically significant increases after five-year pomegranate cultivation.

Copper associated with the less crystalline, amorphous iron fraction emerged as the second most prominent component of extractable copper. Furthermore, its relative distribution in soil increased due to altered field management, rising from approximately 24% to 31.9% in the topsoil layer and to 37.8% in the subsoil layer (Fig. 4). The smallest amount of copper, with concentrations below the quantification limit of the applied analytical method, was found in the water-extractable or exchangeable fraction. This highlights copper's high affinity for soil components and its stability against weak solvents.

Field management changes also caused a significant decrease in the total content of extractable copper, with non-available residual copper increasing from 10.7% to 32.0% at the 50 cm depth. At the 20 cm depth, the conversion to non-extractable copper was less pronounced, with its relative content increasing from 12.4% to 17.6% after five-year pomegranate cultivation.

Distribution of zinc

Altering the field management from rice cultivation to pomegranate cultivation resulted in a decrease in zinc content at both depths, with reductions of 9.1% at 20 cm and 26.9% at 50 cm, closely resembling the effects on copper content in soil (Table 1). However, the patterns of zinc distribution (Fig. 5) differed significantly from those of copper (Fig. 4), as relatively stable zinc associations with manganese and iron in amorphous and crystalline solid phases, as well as with the fraction bound to organic matter and sulphides, were observed regardless the field cultivation.

In both fields, most of zinc was found in the non-available residual fraction, accounting for 54% to 62%, in contrast to the higher leachability of copper. The stability of zinc within the residual fraction was further highlighted by the negligible changes in its relative content even after five years of pomegranate cultivation (Fig. 5). The only zinc fraction in both soil layers that appeared statistically significantly

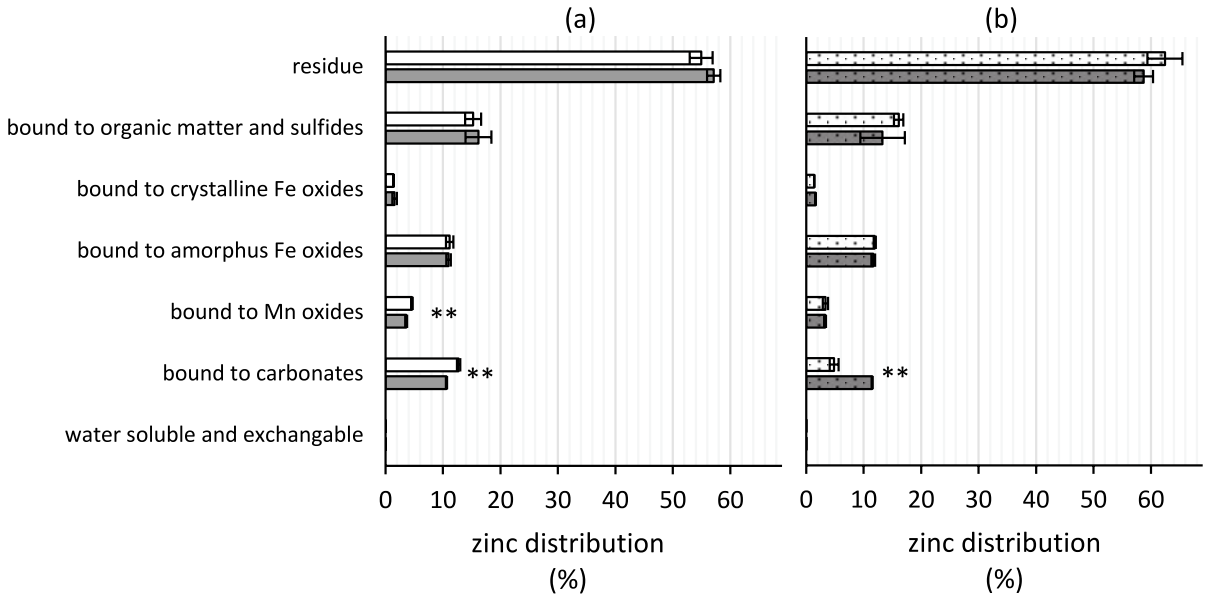

Fig. 5 Distribution of zinc in soils collected at (**a**) 20 cm depth (topsoil sample) (**b**) or 50 cm (subsoil sample). The bars of gray and white colors represent samples collected from the rice field, and the field with five-year pomegranate cultivation after discontinued rice cultivation, respectively (bars represent the mean values, and error bars indicate the standard deviation from three independent, parallel runs; where not visible, error bars are present but too small to be distinguished from the mean value; asterisks show statistically significant differences between samples: * $P < 0.05$, ** $P < 0.01$, and *** $P < 0.001$)

susceptible to changes in soil management was the acid-extractable, carbonate-associated fraction. At the 50 cm depth, this fraction decreased by 57% after five years of pomegranate cultivation. Conversely, at the topsoil layer, the carbonate-associated zinc fraction increased by 20% following changes in soil management.

Similarly to copper, zinc content in the water-extractable and exchangeable fraction was below the quantification limit of the applied analytical method, highlighting its resistance to mobilization when exposed to weak solvents.

Distribution of manganese and aluminum

The distribution patterns of aluminum and manganese revealed two distinct characteristics for each element. The majority of manganese was associated with carbonates, ranging from 74 to 88%, while aluminum was predominantly found in the residual fraction, which accounted for approximately 90% of all aluminum in the soil samples, irrespective of treatment or depth (Fig. 6). The relative content of aluminum within this recalcitrant fraction showed only minor changes. Among the less significant fractions, statistically significant decreases were observed in the carbonate-bound aluminum (from 1.5% to 0.7%) and aluminum associated with amorphous iron minerals (from 3.2% to 2.5%) at the 50 cm depth. These reductions led to the redistribution of aluminum into fractions associated with organic matter and sulfides. A similar, though less pronounced, effect was observed in the topsoil layer (Fig. 6a).

In contrast, manganese relative content in carbonate-bound fraction decreased significantly after five years of pomegranate cultivation. Specifically, at a depth of 50 cm, manganese content dropped by 14%, reaching a final value of 74.4%. The mobilized manganese was primarily redistributed into amorphous and crystalline manganese oxides, as well as the fraction extractable by organic chelates (Fig. 6b). Such alteration in manganese distribution is particularly significant in the context of its total content in the deeper soil layer, which remained unchanged even after changes in field management (Table 1).

On the other hand, the distribution of manganese and its associations with soil components in the topsoil layer did not exhibit drastic changes. There were

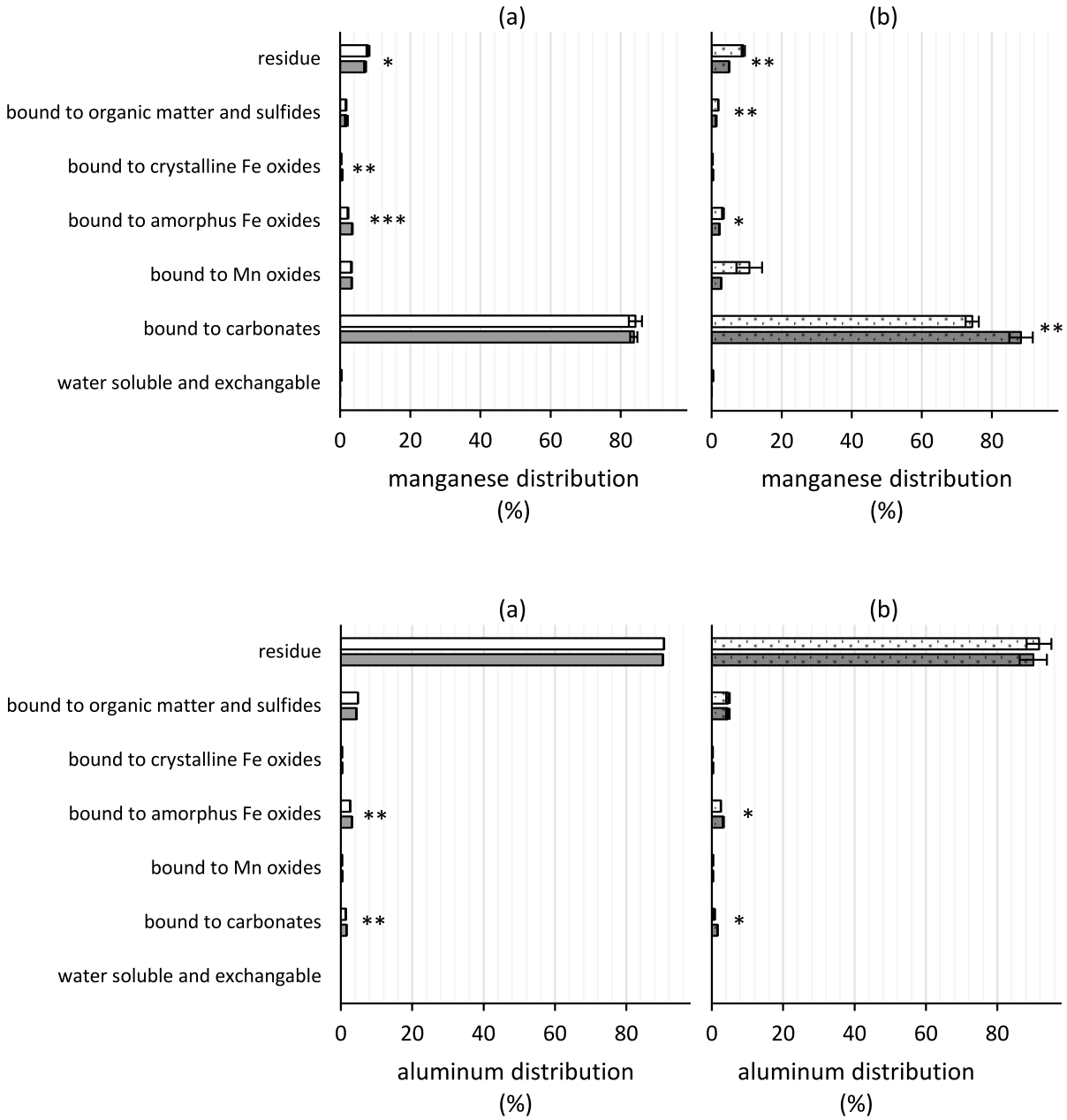

Fig. 6 Distribution of manganese and aluminum in soils collected at (**a**) 20 cm depth (topsoil sample) (**b**) or 50 cm (subsoil sample). The bars of gray and white colors represent samples collected from the rice field, and the field with five-year pomegranate cultivation after discontinued rice cultivation, respectively (bars represent the mean values, and error bars indicate the standard deviation from three independent, parallel runs; where not visible, error bars are present but too small to be distinguished from the mean value; asterisks show statistically significant differences between samples: * $P<0.05$, ** $P<0.01$, and *** $P<0.001$)

no statistically significant alterations in the carbonate-bound fraction, and only the manganese associated with the crystalline and amorphous phases of iron showed a statistically significant decrease, with the combined total of these fractions declining from 4.1% to 2.5%.

Distribution of silicon and phosphorus

Silicon exhibits a relatively uniform response to changes in soil management across the soil horizon. While its content in the topsoil layer decreased by 11%, the subsoil layer at a depth of 50 cm in the pomegranate field exhibited a moderate decrease of 15% (Table 1). This trend mirrored the changes in the content of amorphous silicon (biogenic and nanocrystalline silica) in the topsoil layer, since it was higher for the rice field compared to the pomegranate (Fig. 7).

The alternation in silicon content within fractions extracted using sequential extraction procedure exhibited consistent trends across all soils and depths (Fig. 8). In both fields, the majority of silicon was found in the residual fraction, accounting for more than 80% of the total, irrespective of treatment or depth. A notable portion of silicon was extracted into fraction associated with organic matter and sulfides, ranging from 7 to 8% (Fig. 8). Furthermore, the stability of silicon forms within the soils was confirmed by its low leachability into a 0.01 M $CaCl_2$ solution, representing the bioavailable fraction, which remained below 10 $\mu g \cdot g^{-1}$. Additionally, the amount of silicon extracted by oxalate reaching 200 $\mu g \cdot g^{-1}$ (Table 2), further supporting its stability in the soil.

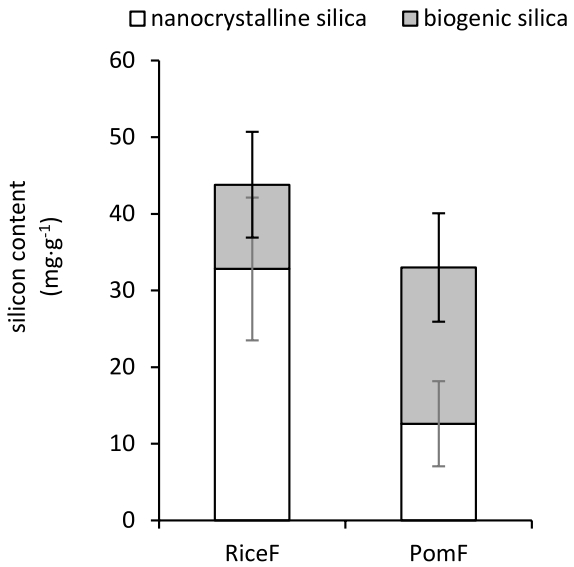

Fig. 7 Distribution of total silicon in amorphous forms (biogenic and nanocrystalline silica) in topsoil samples of rice (RiceF) and pomegranate (PomF) field (bars represent the mean values, and error bars indicate the standard deviation from three independent, parallel runs)

The total phosphorus content in the pomegranate field decreased by 36% at a depth of 50 cm compared to the rice field. In the rice field, the majority of phosphorus was associated with carbonates, ranging from 44 to 49% (Fig. 8). However, after five years of pomegranate cultivation, the relative phosphorus content in the carbonate-bound fraction significantly declined. At 50 cm depth, phosphorus content dropped by more than 70% compared to the rice field. This decrease was accompanied by a partial redistribution of phosphorus into amorphous iron and manganese oxides, while a portion was lost from the soil system, leading to an overall reduction in total phosphorus content in the deeper layer (Fig. 8b). In contrast, phosphorus distribution and its associations with soil components in the topsoil layer remained relatively stable. The only statistically significant change was an increase in phosphorus associated with manganese oxides, rising from 16.8% to 25.1%.

Discussion

Shifts in iron distribution

Among the examined redox-sensitive soil constituents, iron exhibited the most pronounced changes in response to the agricultural transition from rice cultivation to pomegranate farming. Notably, there was a statistically significant reduction in PomF´s total iron content, exceeding 10% (Table 1), accompanied by decreases in both the acid-soluble (carbonate-associated) and the less crystalline, reducible (amorphous iron oxides and oxyhydroxides) fractions (Fig. 2). To interpret these observations, it is essential to consider the unique biogeochemical dynamics within the rhizosphere of rice plants, alongside pedogenic redox-driven processes modulated by microbial activity and fluctuating redox potentials.

The elevated total iron concentrations observed in RiceF soils in comparison to PomF soils (Table 1) likely reflect the efficiency of iron retention under submerged, anoxic conditions occurring through the formation of amorphous ferric oxyhydroxide plaques on rice root surfaces (Liang et al. 2006).

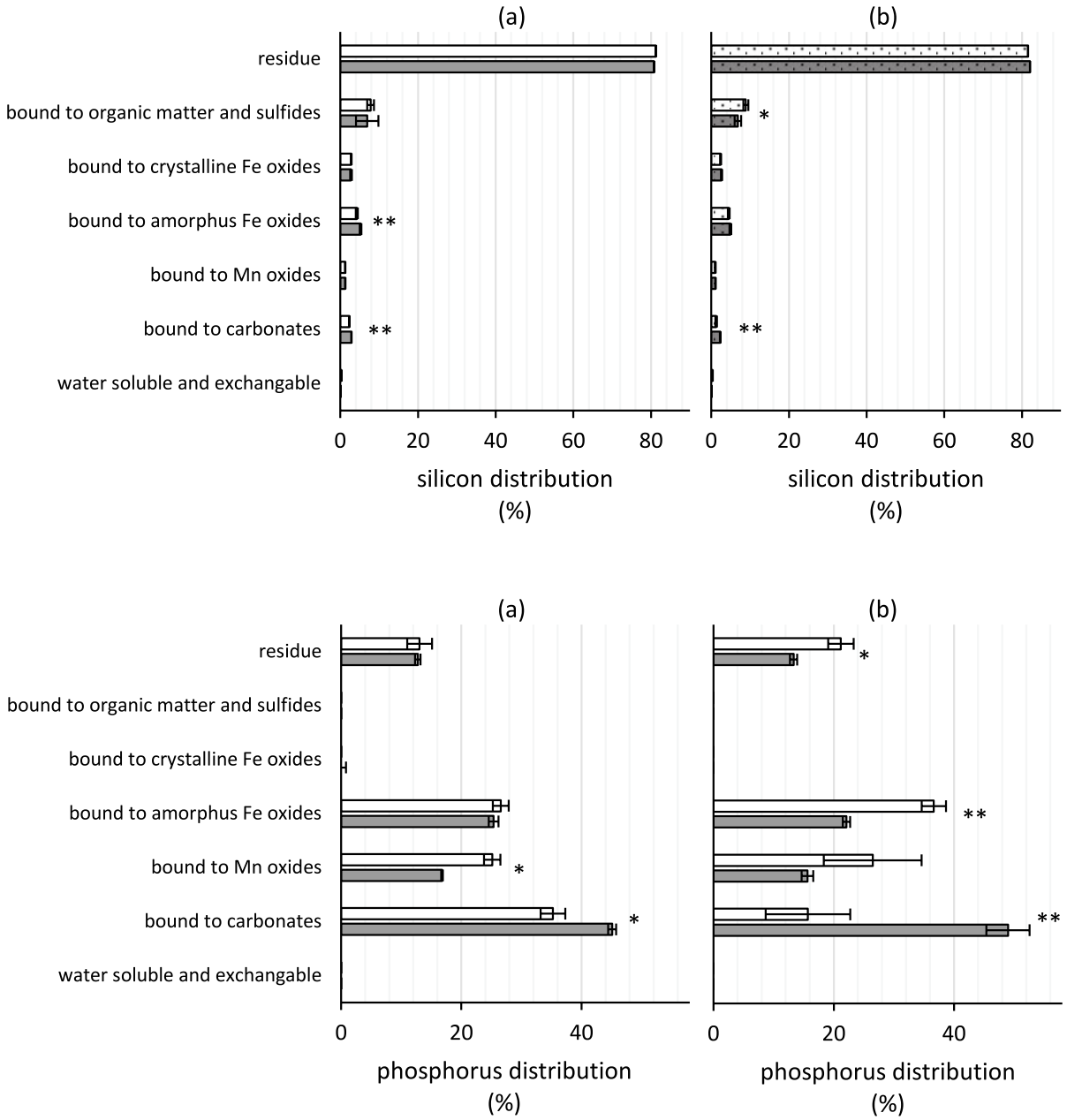

Fig. 8 Distribution of silicon and phosphorus in soils collected at (**a**) 20 cm depth (topsoil sample) (**b**) or 50 cm (subsoil sample). The bars of gray and white colors represent samples collected from the rice field, and the field with five-year pomegranate cultivation after discontinued rice cultivation, respectively (bars represent the mean values, and error bars indicate the standard deviation from three independent, parallel runs; where not visible, error bars are present but too small to be distinguished from the mean value; asterisks show statistically significant differences between samples: * $P<0.05$, ** $P<0.01$, and *** $P<0.001$)

These plaques serve as both reservoirs for sequestered iron and buffers against abiotic stress (Sebastian and Prasad 2016).

The iron plaque predominantly consists of thermodynamically less stable, nanosized crystallites of ferrihydrite ($Fe^{3+}{}_{10}O_{14}(OH)_2$), along with

more crystalline phases such as lepidocrocite (γ-FeO(OH)) and goethite (α-FeO(OH)) (Maisch et al. 2020). Minor levels of siderite ($FeCO_3$) may also be expected, as it commonly occurs on the roots of indigenous wetland plants (Hansel et al. 2001). The stability of these mineral phases is likely a key factor influencing observed changes in iron's distribution (Fig. 2).

Since the early-formed nanosized ferrihydrite precipitates are metastable and susceptible to dissolution following recrystallization process, eventually stabilizing into more ordered and thermodynamically stable goethite (Jambor and Dutrizac 1998), the observed decline in the relative abundance of amorphous iron phases (Fig. 2) suggests that changes in agricultural management reduced the presence of these less crystalline forms. While such conditions might be expected to promote the transformation into more ordered reducible iron oxides, the data indicate that the pool of well-crystallized iron minerals did not significantly increase. This implies that the dissolution of amorphous iron was more pronounced than its remineralization, highlighting a net loss (Table 1) rather than a structural reorganization of the iron phases.

The likely explanation for this phenomenon is a shift in soil microbial composition in response to redox changes, particularly the proliferation of aerobic filamentous fungi. These organisms, which are less adaptable to dynamic redox fluctuations and typically less abundant than bacteria under reducing conditions of paddy soils (Seo and DeLaune 2010), may have contributed to selective dissolution of labile, less-ordered ferric iron phases present on mineral surfaces or comprising iron plaque after transition of pomegranate cultivation. In contrast, the well-crystallized core ferric phases are largely resistant to extracellular enzymatic activity and thus remain relatively unaffected (Miglierini et al. 2021). This selective dissolution could account for the observed depletion of amorphous iron forms without a corresponding increase in more crystalline phases (Fig. 2).

A similar scenario is likely for the carbonate-associated fraction of iron, presumably dominated by siderite ($FeCO_3$) formations. Under oxic conditions at circumneutral to slightly alkaline pH, siderite can undergo oxidative dissolution, leading to the accumulation hydrous ferric oxide transformation products, particularly poorly crystalline and labile ferrihydrite, on carbonate surfaces (Duckworth and Martin 2004).

Resilience of iron valence states

Highlighting the reduction of approximately 97% in acid-soluble fraction, as well as other shifts in iron content and its partitioning (Fig. 2), one would expect this to coincide with significant alterations in its redox state. However, Mössbauer spectroscopy results indicate otherwise (Table 3). The Fe^{2+}/Fe^{3+} ratio remained largely unchanged following the transition to pomegranate cultivation, underscoring the apparent redox stability of iron oxidation states in these soils. Instead of broad redox-driven transformations, only minor structural rearrangements were observed, such as the redistribution of Fe^{3+} within octahedral coordination sites (Table 3).

These results suggest that, despite changes in the hydrological regime and redox potential, iron speciation demonstrates considerable resilience in the experimental fields. Although a shifts toward oxidative conditions, e.g. reoxidation, would typically promote Fe^{3+} dominance (ThomasArrigo and Kretzschmar 2022), studies have shown that cores of mixed-valence or purely ferric/ferrous crystallites exhibit resistance to microbially induced transformations. This is exemplified by observations where the lattice structure of nanosized magnetite, containing mixed iron valences, showed negligible changes even after direct exposure to filamentous fungi under oxic and acidic conditions (Vyhnáleková et al. 2024).

Furthermore, data from Fig. 2 indicate that over 60% of the total iron is sequestered in the residual fraction, which is chemically resistant to acidic, reducing, and oxidizing conditions. This suggests a predominance of silicate-bound or otherwise stable iron compounds, contributing to the persistence of iron valence states within these mineral matrices.

Another contributing factor to the relatively stable iron valence states may be linked to observations by Chen and Thompson (2021), who suggest that coordination of Fe^{2+} with native soil organic matter prior to oxidation is followed by its coprecipitation with newly formed ferric oxides. This process may partially inhibit the rate of Fe^{2+} autocatalytic oxidation by blocking the reactive surfaces of ferric iron oxides, which facilitate electron transfer (Rosso et al. 2010). Consequently, carbon dynamics may have played a

role in stabilizing Fe^{2+} in the soil after changes in cultivation practices.

Carbonate and organic matter dynamics

Iron-organic matter associations help retain both ferrous and ferric iron through coprecipitation with organic matter during the shift to oxic conditions (Sodano et al. 2017). In addition, dissolved organic matter influences the dissolution and phase transformation of iron oxides (Pan et al. 2024). Therefore, these processes should be considered crucial for iron and related elements' dynamics in organic-rich paddy soils, especially following the transition to permanently oxidative farming regime during pomegranate cultivation.

High organic carbon content in soils is often considered the main factor preventing ferrihydrite transformation into more thermodynamically stable phases (Kalbitz et al. 2005). As a result, the persistence of poorly crystalline ferrihydrite should provide a larger reactive surface area for the immobilization of metals and metalloids, compared to well-crystallized phases such as goethite (Tang et al. 2025). However, since our results are indicative of decrease in amorphic ferrous and ferric phases after changes in soil management from rice to pomegranate (Fig. 2) while organic carbon content increases (Table 1), the carbon dynamics should have been altered in such a way that inhibits ferrihydrite stabilization. In the topsoil, this effect is complex but can be explained.

We hypothesized that the change in cultivation and soil management led to shifts in microbial populations, e.g. fungi, mycorrhizal fungi or bacteria, which are capable of organic carbon mineralization from weak early-formed amorphous mineral-organic matter associations (Bölscher et al. 2025). This, in turn, increased iron availability and promoted its dissolution, likely due to elevated production of chelating agents of microbial origin (Li et al. 2018), as indicated by the rise in dissolved organic matter content (Table 1). The subsequent stabilization of populations and increased carbon utilization efficiency also contributes to the accumulation of residual biomass and organic matter (Martí-Roura et al. 2019), which likely has a lower capacity to stabilize poorly crystalline iron phases, but serves as a new pool of organic carbon in the soil.

The newly formed organic matter may have also established more stable associations with secondary calcium carbonates (Virto et al. 2018), whose content in the soil increased significantly after changes in soil management (Table 1). Indeed, Rovira and Vallejo (2008) reported that intensified soil respiration can lead to a significant increase in carbonate content. Furthermore, the increase in exchangeable calcium is known to promote the growth and activity of surface-adhering populations (Shabtai et al. 2023). Therefore, the elevated calcium carbonate (Table 1) and water exchangeable calcium levels (Table 2) observed after the transition in soil management may indirectly reflect enhanced soil microbial activity.

In the subsoil layer, an intensified initial mineralization of organic carbon likely occurred to some extent after changes in management (e.g., increased calcium carbonate content), with similar outcome related to iron, as suggested by the observed decrease in its total content (Table 1). However, we hypothesize that the microbial community composition remained relatively resilient towards the changes in farming, and the lack of additional carbon input following the shift in soil management likely contributed to the statistically significant decline in both soil organic carbon and dissolved organic matter. The distinct redistribution of iron, particularly its apparent increased association with the residual fraction, suggests that microbial processes at depths below 50 cm may follow different strategies compared to those in topsoils. Unfortunately, overall microbial activity was not assessed in this study; therefore, the direct influence of microbial processes on organic carbon dynamics and mineral transformations could not be confirmed.

Shifts in copper distribution and stability of zinc

The transition from flooded rice cultivation to non-flooded pomegranate cultivation significantly affected the total concentrations and solid-phase distribution of copper and zinc, particularly in the subsoil layers (Table 1). Despite the observed decrease, the total copper and zinc contents in the topsoil remained slightly above the average levels reported for Italy. Since both elements are typically accumulated in the Ap horizon (Bini et al. 1988), their lower concentrations in the subsoils were anticipated.

Overall, the results on copper and zinc partitioning highlight their contrasting responses to changes in agricultural management and soil aging. Copper demonstrates high mobility under fluctuating redox conditions, showing significant redistribution among reactive fractions (Fig. 4), whereas zinc displays greater stability, with only minor changes observed in its most labile forms (Fig. 5).

It has been reported that copper is highly sensitive to variations in manganese and iron mineral soil constituents and organic matter content, and it tends to redistribute into more labile fractions in response to redox fluctuations (Balint et al. 2015). As the soil organic matter and oxygenated ferrous and ferric phase transformations are key factors influencing copper mobility, particularly at circumneutral pH (Seda et al. 2016), the changes in redox dynamics following the transition to pomegranate cultivation likely played a significant role in copper redistribution (Fig. 4). Indeed, except the fraction bound to amorphous phases, the pattern of copper distribution closely resembles that of iron (Fig. 2). Thus, similarly to iron distributions, the most sensitive to changes in soil management was the fraction associated with carbonates (acid-soluble fraction).

In calcareous soils, the precipitation of $CuCO_3$ on calcite ($CaCO_3$) surfaces is considered a primary retention mechanism (Ponizovsky et al. 2007), particularly in systems with high solution-to-soil ratios (Rodriguez-Rubio et al. 2003), which to some extent resembles the conditions in paddy soils. Therefore, the elevated levels of copper associated with the carbonate fraction were not unexpected. However, the extent of copper depletion from the carbonate-associated fraction in both topsoil and subsoil was unprecedented in our experience (Fig. 4).

Given that calcite has a higher dissolution constant and copper carbonates are generally less sensitive to CO_2 partial pressure and low pH, it is likely that other acid-soluble forms of copper were responsible for this loss (Fig. 4). Cui et al. (2019) reported, based on XANES analysis of paddy soils, that copper is primarily associated with ferrihydrite, goethite, or sulfides. As previously discussed, ferrihydrite can form on calcite surfaces in paddy soils but is prone to selective dissolution under oxic conditions by microorganisms. We hypothesize that this dissolution process may contribute to the observed decrease in the acid-soluble (carbonate-associated) copper fraction in PomS soil samples. This could be due to copper being sorbed to labile ferrihydrite phases via inner-sphere, bidentate surface complexation, involving $Fe(OOH)_6$ polyhedra and square-planar $(CuO_4H_n)^{n-6}$ species (Moon and Peacock 2012). The desorption of copper from these complexes can be facilitated by high concentrations of water-soluble Ca^{2+} ions as well as low-molecular-weight organic compounds, which are key components of dissolved organic matter (Seda et al. 2016). These constituents are also prevalent in our topsoil samples (Table 1), potentially enhancing copper mobility.

Once released from the carbonate-associated fraction due to changes in soil management, copper was likely redistributed onto surfaces of ferric hydrated oxides and oxohydroxides, and organic matter (Jönsson et al. 2006), as evidenced by the observed changes in our experiment (Fig. 4), which provide the high affinity sorption sites.

The substantial shift of copper from the carbonate-associated fraction toward organic and iron-associated fractions in the subsoil following changes in cultivation can be further supported by the observed redistribution of manganese (Fig. 6). Iron oxides are known to catalyze the oxidation of manganese(II), which is in our case likely associated with carbonate complexes, leading to the formation of Mn-bearing oxides (Hu et al. 2023). The reductive dissolution of ferrihydrite formed on carbonate mineral surfaces, coupled with the subsequent oxidation and precipitation of dissolved manganese into higher-valence oxides (reducible fraction), as observed in Fig. 6, likely facilitates the depletion of copper from the carbonate-associated fraction (Fig. 4). However, this manganese-related process appears to be inhibited in the topsoil, likely due to the increased concentration of dissolved organic matter, which significantly suppresses this catalytic activity, particularly in the presence of ferrihydrite (Huang et al. 2025).

In contrast to complex changes of copper distribution, zinc showed greater geochemical stability. Although total zinc content declined similarly to copper (Table 1), its redistribution among fractions was minimal. Zinc remained predominantly bound in the residual fraction (Fig. 5) across both soil layers, regardless of cultivation history. This fraction is considered non-bioavailable and strongly bound within the mineral matrix, highlighting zinc's resistance to mobilization and redistribution over short-term land

use changes (Wisawapipat et al. 2017). Our results agree with previous studies, which documented the residual fractions to represent the largest zinc concentrations and are incorporated in stable zinc-containing minerals (Kashem et al. 2007).

Conclusions

This study highlights how changes in cultivation practices, from flooded rice fields to non-flooded pomegranate orchards, influence iron speciation, organic matter dynamics, and trace metal distribution in calcareous, organic-rich soils. We show that the transition to oxic conditions leads to the destabilization of amorphous iron phases, likely driven by shifts in microbial activity and carbon mineralization pathways. These processes, in turn, affect the mobility and partitioning of trace elements such as copper and zinc, with copper exhibiting pronounced redistribution, particularly from carbonate-associated to organic and iron-bound fractions. Understanding the interactions between iron mineral phases and change in cultivation method offers valuable insights for mechanisms, controlling nutrient availability or contaminant mobility under different farming regimes. These finding have important implications for sustainable agriculture and soil management. By recognizing how change in soil cultivation effects the micronutrient dynamics, speciation and mobility of elements can lead to better tailor practices to maintain soil health, enhance nutrient retention and reduce metal leaching risks. Our research can support the development of strategies for improving soil fertility in organic rich systems for optimizing land use transitions from rice to other crops, without losing agricultural productivity.

Acknowledgements This work was supported by the Scientific Grant Agency of the Slovak Republic Ministry of Education and the Slovak Academy of Sciences under VEGA contract Nos. 1/0175/22, 1/0139/22, and 1/0010/24, and by the Large Research Infrastructures of the Ministry of Education, Youth and Sports of the Czech Republic: LM2023073. The authors are grateful to dr. Benito Scazziota (Società Agricola Terzeria Srl Soc. Benefit, Francavilla Marittima, CS, Italy) for farm access and having generously hosted the field trial.

Author contributions All authors contributed to the study conception and design. Material preparation, data collection and analysis were performed by Veronika Cyprichová, Antonio Gelsomino, Marek Bujdoš, Beatrix Petrovičová and Martin Urík. The first draft of the manuscript was written by Veronika Cyprichová and all authors commented on previous versions of the manuscript. All authors read and approved the final manuscript.

Funding Open access funding provided by The Ministry of Education, Science, Research and Sport of the Slovak Republic in cooperation with Centre for Scientific and Technical Information of the Slovak Republic.

Data availability Data are available through Mendeley Data at https://doi.org/10.17632/dz35z5kvm3.1

Declarations

Competing interests The authors have no relevant financial or non-financial interests to disclose.

Open Access This article is licensed under a Creative Commons Attribution 4.0 International License, which permits use, sharing, adaptation, distribution and reproduction in any medium or format, as long as you give appropriate credit to the original author(s) and the source, provide a link to the Creative Commons licence, and indicate if changes were made. The images or other third party material in this article are included in the article's Creative Commons licence, unless indicated otherwise in a credit line to the material. If material is not included in the article's Creative Commons licence and your intended use is not permitted by statutory regulation or exceeds the permitted use, you will need to obtain permission directly from the copyright holder. To view a copy of this licence, visit http://creativecommons.org/licenses/by/4.0/.

References

Alan M, Kara D (2019) Comparison of a new sequential extraction method and the BCR sequential extraction method for mobility assessment of elements around boron mines in Turkey. Talanta 194:189–198. https://doi.org/10.1016/j.talanta.2018.10.030

Balint R, Said-Pullicino D, Ajmone-Marsan F (2015) Copper dynamics under alternating redox conditions is influenced by soil properties and contamination source. J Contam Hydrol 173:83–91. https://doi.org/10.1016/j.jconhyd.2014.12.003

Bini C, Dall'Aglio M, Ferretti O, Gragnani R (1988) Background levels of microelements in soils of Italy. Environ Geochem Health 10:63–69. https://doi.org/10.1007/BF01758593

Bölscher T, Cardon ZG, Garcia Arredondo M, Grand S, Griffen G, Hestrin R, Imboden J, Jamoteau F, Lacroix EM, Pérez Castro S, Persson P, Riley WJ, Keiluweit M (2025) Vulnerability of mineral-organic associations in the rhizosphere. Nat Commun 16:5527. https://doi.org/10.1038/s41467-025-61273-4

Cui J-l, Zhao Y-p, Lu Y-J, Chan T-s, Zhang L-l, Tsang DCW, Li X-d (2019) Distribution and speciation of copper in rice (*Oryza sativa* L.) from mining-impacted paddy soil: implications for copper uptake mechanisms. Environ Int 126:717–726. https://doi.org/10.1016/j.envint.2019.02.045

DeMaster DJ (1981) The supply and accumulation of silica in the marine environment. Geochim Cosmochim Acta 45:1715–1732

Duckworth OW, Martin ST (2004) Role of molecular oxygen in the dissolution of siderite and rhodochrosite1 1Associate editor: U Becker. Geochimica Et Cosmochimica Acta 68:607–621. https://doi.org/10.1016/S0016-7037(03)00464-2

Hagarová I (2015) Extractions complying with the principles of green chemistry used in trace analysis of metals. Chem Listy 109:269–275

Hansel CM, Fendorf S, Sutton S, Newville M (2001) Characterization of Fe plaque and associated metals on the roots of mine-waste impacted aquatic plants. Environ Sci Technol 35:3863–3868. https://doi.org/10.1021/es0105459

Haysom MBC, Chapman LS (1975) Some aspects of the calcium silicate trials at Mackay. Proceedings of the 42nd Conference, Queensland Society of Sugar Cane Technologists. Australian Society of Sugar Cane Technologists, Bundaberg.

Hu N, Li Z, Huang P, Tao C (2006) Distribution and mobility of metals in agricultural soils near a copper smelter in South China. Environ Geochem Health 28:19–26. https://doi.org/10.1007/s10653-005-9007-z

Hu S, Zheng L, Zhang H, Chen G, Yang Y, Ouyang Z, Chen S, Gao K, Liu C, Wang Q, Liu T (2023) Hematite-mediated Mn(II) abiotic oxidation under oxic conditions: pH effect and mineralization. J Colloid Interface Sci 636:267–278. https://doi.org/10.1016/j.jcis.2023.01.034

Huang X, Yang B, Dou Y, Ding Y (2025) Coupled transformations of manganese and dissolved organic matter molecules during iron (oxyhydr)oxide-catalyzed oxidation of Mn(II). J Environ Sci (China) 155:538–551. https://doi.org/10.1016/j.jes.2024.07.012

Chen C, Thompson A (2021) The influence of native soil organic matter and minerals on ferrous iron oxidation. Geochim Cosmochim Acta 292:254–270. https://doi.org/10.1016/j.gca.2020.10.002

Jambor JL, Dutrizac JE (1998) Occurrence and constitution of natural and synthetic ferrihydrite, a widespread iron oxyhydroxide. Chem Rev 98:2549–2585. https://doi.org/10.1021/cr970105t

Jönsson J, Sjöberg S, Lövgren L (2006) Adsorption of Cu(II) to schwertmannite and goethite in presence of dissolved organic matter. Water Res 40:969–974. https://doi.org/10.1016/j.watres.2006.01.006

Kalbitz K, Schwesig D, Rethemeyer J, Matzner E (2005) Stabilization of dissolved organic matter by sorption to the mineral soil. Soil Biol Biochem 37:1319–1331. https://doi.org/10.1016/j.soilbio.2004.11.028

Kashem MA, Singh BR, Kondo T, Imamul Huq SM, Kawai S (2007) Comparison of extractability of Cd, Cu, Pb and Zn with sequential extraction in contaminated and non-contaminated soils. Int J Environ Sci Technol 4:169–176. https://doi.org/10.1007/BF03326270

Klute A (1986) Methods of soil analysis, 2nd edn. American Society of Agronomy

Kögel-Knabner I, Amelung W, Cao Z, Fiedler S, Frenzel P, Jahn R, Kalbitz K, Kölbl A, Schloter M (2010) Biogeochemistry of paddy soils. Geoderma 157:1–14. https://doi.org/10.1016/j.geoderma.2010.03.009

Li F, Koopal L, Tan W (2018) Roles of different types of oxalate surface complexes in dissolution process of ferrihydrite aggregates. Sci Rep 8:2060. https://doi.org/10.1038/s41598-018-20401-5

Liang Y, Zhu YG, Xia Y, Li Z, Ma Y (2006) Iron plaque enhances phosphorus uptake by rice (*Oryza sativa*) growing under varying phosphorus and iron concentrations. Ann Appl Biol 149:305–312. https://doi.org/10.1111/j.1744-7348.2006.00095.x

Liu R, Altschul EB, Hedin RS, Nakles DV, Dzombak DA (2014) Sequestration enhancement of metals in soils by addition of iron oxides recovered from coal mine drainage sites. Soil Sediment Contam 23(4):374–388. https://doi.org/10.1080/15320383.2014.831027

Maisch M, Lueder U, Kappler A, Schmidt C (2020) From plant to paddy—how rice root iron plaque can affect the paddy field iron cycling. Soil Syst. https://doi.org/10.3390/soilsystems4020028

Martí-Roura M, Hagedorn F, Rovira P, Romanyà J (2019) Effect of land use and carbonates on organic matter stabilization and microbial communities in Mediterranean soils. Geoderma 351:103–115. https://doi.org/10.1016/j.geoderma.2019.05.021

Miglierini MB, Dekan J, Urík M, Cesnek M, Kmječ T, Matúš P (2021) Fungal-induced modification of spontaneously precipitated ochreous sediments from drainage of abandoned antimony mine. Chemosphere 269:128733. https://doi.org/10.1016/j.chemosphere.2020.128733

Moon EM, Peacock CL (2012) Adsorption of Cu(II) to ferrihydrite and ferrihydrite–bacteria composites: importance of the carboxyl group for Cu mobility in natural environments. Geochim Cosmochim Acta 92:203–219. https://doi.org/10.1016/j.gca.2012.06.012

Nemček L, Hagarová I (2021) The recent strategies employed in chemical analysis of contaminated waters, sediments and soils as a part of the remediation process: Extraction. In: R Prasad (ed) Environmental Pollution and Remediation. Springer Singapore, Singapore

Nishimura S, Yonemura S, Sawamoto T, Shirato Y, Akiyama H, Sudo S, Yagi K (2008) Effect of land use change from paddy rice cultivation to upland crop cultivation on soil carbon budget of a cropland in Japan. Agric Ecosyst Environ 125:9–20. https://doi.org/10.1016/j.agee.2007.11.003

Notini L, Schulz K, Kubeneck LJ, Grigg ARC, Rothwell KA, Fantappiè G, ThomasArrigo LK, Kretzschmar R (2023) A new approach for investigating iron mineral transformations in soils and sediments using ^{57}Fe-labeled minerals and ^{57}Fe Mössbauer spectroscopy. Environ Sci Technol 57:10008–10018. https://doi.org/10.1021/acs.est.3c00434

Pan X, Huang X, Deng N (2024) The fate of cadmium during ferrihydrite phase transformation affected by dissolved organic matter: insights from organic-mineral interaction. Chem Geol 670:122424. https://doi.org/10.1016/j.chemgeo.2024.122424

Ponizovsky AA, Allen HE, Ackerman AJ (2007) Copper activity in soil solutions of calcareous soils. Environ Pollut 145:1–6. https://doi.org/10.1016/j.envpol.2006.04.010

Raimondo ML, Lops F, Tarantino A, Bellantuono N, Carlucci A, Bimbo F (2025) The current state of Italian pomegranate production: agronomic, crop protection, economic, and managerial perspectives. Agronomy. https://doi.org/10.3390/agronomy15040826

Rodriguez-Rubio P, Morillo E, Madrid L, Undabeytia T, Maqueda C (2003) Retention of copper by a calcareous soil and its textural fractions: influence of amendment with two agroindustrial residues. Eur J Soil Sci 54:401–409. https://doi.org/10.1046/j.1365-2389.2003.00529.x

Rosso KM, Yanina SV, Gorski CA, Larese-Casanova P, Scherer MM (2010) Connecting observations of hematite (alpha-Fe2O3) growth catalyzed by Fe(II). Environ Sci Technol 44:61–67. https://doi.org/10.1021/es901882a

Rovira P, Vallejo VR (2008) Changes in δ13C composition of soil carbonates driven by organic matter decomposition in a Mediterranean climate: a field incubation experiment. Geoderma 144:517–534. https://doi.org/10.1016/j.geoderma.2008.01.006

Sebastian A, Prasad MNV (2016) Iron plaque decreases cadmium accumulation in *Oryza sativa* L. and serves as a source of iron. Plant Biol 18:1008–1015. https://doi.org/10.1111/plb.12484

Seda NN, Koenigsmark F, Vadas TM (2016) Sorption and coprecipitation of copper to ferrihydrite and humic acid organomineral complexes and controls on copper availability. Chemosphere 147:272–278. https://doi.org/10.1016/j.chemosphere.2015.12.106

Seo DC, DeLaune RD (2010) Effect of redox conditions on bacterial and fungal biomass and carbon dioxide production in Louisiana coastal swamp forest sediment. Sci Total Environ 408:3623–3631. https://doi.org/10.1016/j.scitotenv.2010.04.043

Shabtai IA, Wilhelm RC, Schweizer SA, Höschen C, Buckley DH, Lehmann J (2023) Calcium promotes persistent soil organic matter by altering microbial transformation of plant litter. Nat Commun 14:6609. https://doi.org/10.1038/s41467-023-42291-6

Sodano M, Lerda C, Nisticò R, Martin M, Magnacca G, Celi L, Said-Pullicino D (2017) Dissolved organic carbon retention by coprecipitation during the oxidation of ferrous iron. Geoderma 307:19–29. https://doi.org/10.1016/j.geoderma.2017.07.022

Sparks DL, Page AL, Helmke PA (2001) Methods of soil analysis chemical methods

Tamm O (1922) Om bestämning av de oorganiska komponenterna i markens gelkomplex. Medd Statens Skogsfoersoeksanst 19:385–404

Tang N, Siebers N, Dultz S, Klumpp E (2025) Elucidating the role of ferrihydrite and goethite in the aggregation and stability of small soil microaggregates: an experimental study on arable Luvisols under different management. Geoderma 459:117351. https://doi.org/10.1016/j.geoderma.2025.117351

ThomasArrigo LK, Kretzschmar R (2022) Iron speciation changes and mobilization of colloids during redox cycling in Fe-rich, Icelandic peat soils. Geoderma 428:116217. https://doi.org/10.1016/j.geoderma.2022.116217

Virto I, Antón R, Apesteguía M, Plante A (2018) Chapter 9 - Role of carbonates in the physical stabilization of soil organic matter in agricultural mediterranean soils. In: MÁ Muñoz, R Zornoza (eds) Soil Management and Climate Change. Academic Press

Vyhnáleková S, Miglierini MB, Dekan J, Bujdoš M, Dobročka E, Farkas B, Matúš P, Urík M (2024) Encapsulating magnetite nanopowder with fungal biomass: investigating effects on chemical and mineralogical stability. Sep Purif Technol 333:125899. https://doi.org/10.1016/j.seppur.2023.125899

Wisawapipat W, Janlaksana Y, Christl I (2017) Zinc solubility in tropical paddy soils: a multi-chemical extraction technique study. Geoderma 301:1–10. https://doi.org/10.1016/j.geoderma.2017.04.002

Yang D, Zhang M (2014) Effects of land-use conversion from paddy field to orchard farm on soil microbial genetic diversity and community structure. Eur J Soil Biol 64:30–39. https://doi.org/10.1016/j.ejsobi.2014.07.003

Publisher's Note Springer Nature remains neutral with regard to jurisdictional claims in published maps and institutional affiliations.